

## Effect of Pore Confinement and Molecular Orientation on Hydrogen Transfer during a Free-Radical Reaction in Mesoporous Silica

Michelle K. Kidder and A. C. Buchanan, III\*

Chemical Sciences Division, Oak Ridge National Laboratory, Bethel Valley Road,  
Oak Ridge, Tennessee 37831-6197

Received: October 5, 2007; In Final Form: November 20, 2007

Mesoporous silicas with controllable pore size are providing important platforms finding a multitude of applications such as in catalysis, separations, and as nanoreactors for molecular transformations. In this study, we probe the influence of a coattached hydrogen donor molecule, fluorene, on the free-radical pyrolysis of 1,3-diphenylpropane (DPP) in MCM-41 silica as a function of pore size (1.6–2.8 nm). The influence of surface orientation of the fluorene molecule on the pyrolysis rate is examined through use of isomeric 2-hydroxyfluorene (2-FL) and 3-hydroxyfluorene (3-FL) precursors for surface attachment. The DPP pyrolysis rates are found to be sensitive to both the surface orientation of the fluorene molecule and the pore size. Furthermore, whereas the 2-FL led to faster DPP pyrolysis rates compared with 3-FL on the exterior surface of a nonporous silica nanoparticle (Cabosil), the opposite effect was observed in the mesoporous silica with the smallest pore size. The results are interpreted based on the influence of molecular orientation of the isomeric fluorene molecules on the key bimolecular hydrogen transfer steps to intermediate free-radicals on the surface and suggest that differences in surface curvature between the Cabosil particles and MCM-41 cylindrical pores may play a key role.

### Introduction

Chemical transformations on surfaces are important in many research areas such as catalysis, separations, solid-phase synthesis, and sensor design. Of particular current interest is the effect of nanoconfinement, for example in mesoporous silicas, on chemical properties and reactivity of organic molecules with applications to drug delivery, solid-phase organic synthesis, chiral catalysis, and synthesis of novel materials.<sup>1–6</sup> We recently began exploring confinement effects on organic free-radical reactions at elevated temperatures through the use of covalently immobilized molecules in the pores of hexagonal mesoporous silicas MCM-41 and SBA-15.<sup>7–9</sup> These silicas are attractive because of their high surface areas, ordered pore structures, and tunable pore sizes.<sup>10,11</sup> When compared with the corresponding chemical transformations occurring on nonporous silica, such as Cabosil fumed silica, the effects of the pore environment and pore size can be revealed. For example, in the pyrolysis of phenethyl phenyl ether (PPE) tethered in mesoporous silicas, we recently observed a significant change in product selectivity resulting from steric effects in the crowded pore environment compared with the case of PPE tethered to Cabosil.<sup>9</sup>

The surface attachment method employed for our pyrolysis studies involves condensation of aromatic phenols with the silica surface silanols resulting in a thermally robust Si–O–C<sub>aryl</sub> linkage to the surface.<sup>7–9,12</sup> This permits great flexibility in tailoring the structure of the interface including the use of more than one component, as well as the ability to change the orientation of a given molecule on the surface through control over the position of the phenol functional group in the precursor molecule (e.g., with ortho-, meta-, and para-substituted phenols).<sup>12,13</sup> Since the surface linkage is hydrolytically unstable,

surface-bound pyrolysis products can be easily detached chemically and recovered for quantitative analysis. In the current study, we probe the influence of a coattached hydrogen donor molecule, fluorene, on pyrolysis of 1,3-diphenylpropane (DPP) in MCM-41 silica as a function of pore size (1.6–2.8 nm). In particular, we compare the influence of orientation of the fluorene molecule on the surface through use of isomeric 2-hydroxyfluorene and 3-hydroxyfluorene precursors, as well as the influence of pore confinement through comparison with corresponding studies utilizing nonporous Cabosil nanoparticles.

DPP is an excellent probe molecule for this study since its pyrolysis products are simple (Figure 1a) and the free radical chain decomposition mechanism is well-understood.<sup>7</sup> The propagation steps are shown in Figure 1b. The DPP pyrolysis rate is determined by the rates of the bimolecular hydrogen transfer steps (eq 1) involving the chain carrying gas-phase and surface-attached benzyl radicals since the subsequent unimolecular  $\beta$ -scission steps (eqs 2 and 3) are much faster. The reaction occurs in a similar fashion in mesoporous silicas as on Cabosil, although the pyrolysis rate is enhanced in the confined environment of the mesoporous silicas.<sup>7a</sup>

In prior studies on Cabosil, the DPP pyrolysis rate was very sensitive to the presence of intervening spacer molecules.<sup>13</sup> For example, the DPP rate was ca. 35-times faster in the presence of coattached diphenylmethane molecules than for coattached biphenyl molecules at similar surface coverages. This behavior was unique to the surface-confined environment, and detailed kinetic studies revealed the occurrence of a hydrogen transfer, radical relay process in the presence of hydrogen donor molecules which overcomes diffusional constraints normally imposed on bimolecular surface reactions by immobilization (Figure 2).<sup>13</sup> Recent studies showed that hydroaromatic molecules such as tetralin, 9,10-dihydrophenanthrene, and fluorene, in which the benzylic hydrogens are locked in a ring, are still

\* Author to whom correspondence should be addressed. Phone: (865) 576-2168. Fax: (865) 576-7956. E-mail: buchananac@ornl.gov.

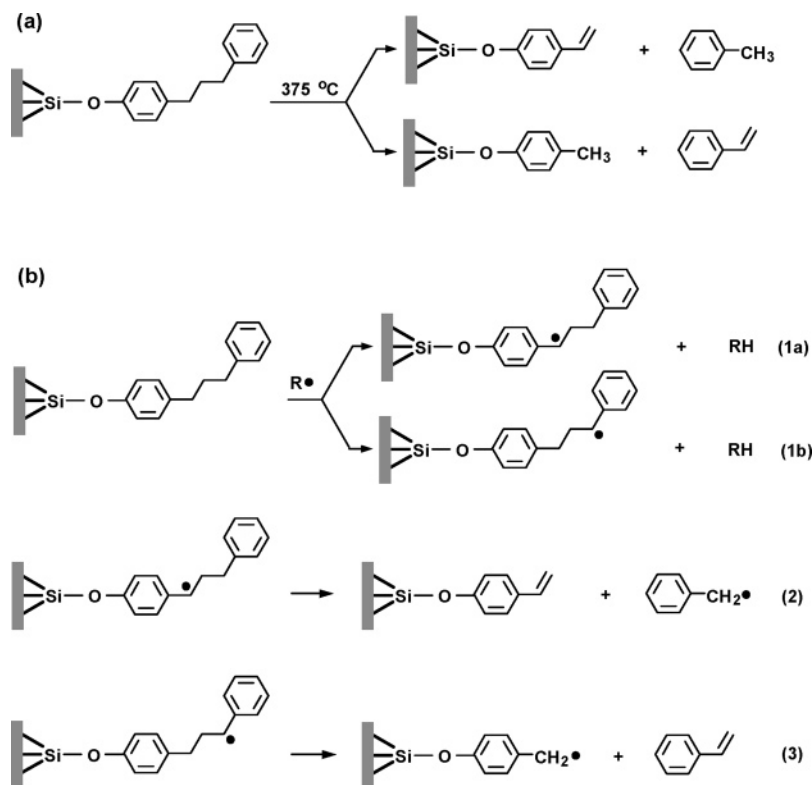


**Figure 1.** (a) Pyrolysis products for silica-confined DPP. (b) Radical chain propagation steps.

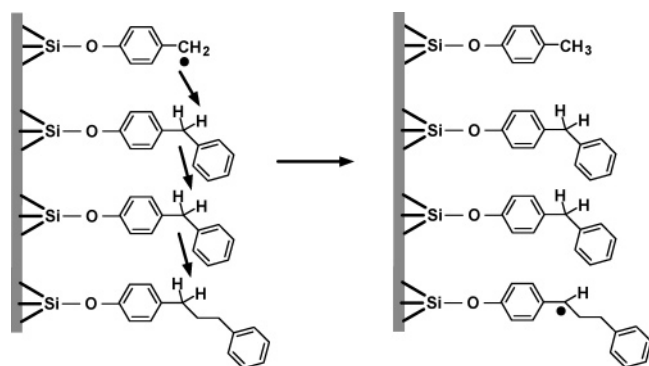


**Figure 2.** Hydrogen transfer, radical relay pathway with diphenylmethane spacer molecule.

effective hydrogen donors.<sup>12</sup> However, examination of isomers of the hydrogen donors revealed sensitivity of the DPP pyrolysis rate to the orientation of the hydroaromatic spacer molecule on the surface,<sup>12</sup> which will be discussed below in comparison with results from the MCM-41 mesoporous silicas.

## Experimental Section

BET specific surface areas were obtained from nitrogen adsorption–desorption isotherms measured at 77 K on a Quantochrome Autosorb-1-C analyzer with all samples outgassed at 100 °C for 6 h prior to analysis. Native mesoporous silicas were also dried at 200 °C for 4 h before outgassing. Pore size distributions were analyzed by the BJH method. GC analyses were performed on a Hewlett-Packard 5890 Series II gas chromatograph employing a J & W Scientific 30 m × 0.25 mm DB-5 column (0.25 μm film thickness) and flame ionization detection. Detector response factors were determined relative to cumene (hydrocarbon products) or 2,5-dimethylphenol and *p*-hydroxybiphenyl (phenolic products) as internal standards. Mass spectra were obtained at 70 eV with an Agilent 6890N/

5973 GC-MS equipped with a capillary column matched to that used for GC analyses.

**Preparation of Surface-Attached Materials.** Two MCM-41 samples with pore diameters of 2.8 nm (913 m<sup>2</sup> g<sup>-1</sup>) and 1.6 nm (1120 m<sup>2</sup> g<sup>-1</sup>) were prepared as previously reported.<sup>7a</sup> The syntheses of 2-hydroxyfluorene (2-HOFL), 3-hydroxyfluorene (3-HOFL), and *p*-(3-phenylpropyl)phenol (HODPP) have also been reported.<sup>12a</sup> The two-component surfaces were prepared at saturation surface coverage in a similar fashion to that reported for DPP<sup>7</sup> by the cocondensation of the HOFL spacer and HODPP (ca. 3:1 mol ratio) with the surface silanols. For example, MCM-41 (2.8 nm) was dried in an oven at 200 °C for 4 h and then cooled in a desiccator. The MCM-41 (1.0 g, ca. 3.8 mmol SiOH assuming a maximum of ca. 2.5 SiOH nm<sup>-2</sup> are derivatizable<sup>7,14</sup>), HOFL (0.725 g, 4.0 mmol), and HODPP (0.303 g, 1.43 mmol) were slurried in dry benzene (20 mL) after which the benzene was removed via rotovap. The attachment reaction took place in a sealed, evacuated tube (5 × 10<sup>-6</sup> Torr) in a sand bath at 225 °C for 1 h. Excess phenolic material was removed via sublimation in a tube furnace at 225–275 °C where the temperature was increased in 10 °C increments every 10 min until 275 °C, where it was held for 20 min. Surface coverage analysis involved an aqueous base hydrolysis procedure and GC quantification with the use of internal standards.<sup>7</sup> The samples were stored in a vacuum desiccator.

**Pyrolysis Procedure.** Pyrolysis experiments were conducted in a three-zone tube furnace (±1 °C) on 50–70 mg samples contained in evacuated and sealed (5 × 10<sup>-6</sup> Torr) T-shaped tubes as previously described.<sup>7</sup> Gas-phase products were collected in a cold trap (77 K) and analyzed by GC and GC-MS with internal standards. Surface-attached products were analyzed in a similar fashion following cleavage from the silica surface by an aqueous base hydrolysis procedure, which liberates these products as phenols.<sup>7</sup> The product mixture was dominated by the four products shown in Figure 1a. Products resulting from addition of the intermediate fluorenyl radicals to the surface-

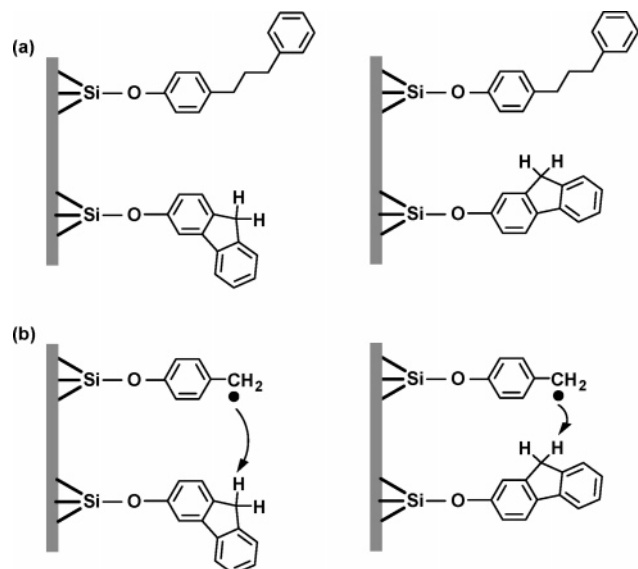


**Figure 3.** (a) MCM-41 confined samples of DPP with 3-fluorene (left) and 2-fluorene (right) spacer molecules. (b) Key hydrogen transfer step where molecular orientation plays a pivotal role.

**TABLE 1: DPP Pyrolysis Rate at 375 °C as a Function of Silica Support and Structure of Hydrogen Donating Spacer Molecule**

silica <sup>a</sup>	surface composition <sup>b</sup>	graft density <sup>c</sup> (nm <sup>-2</sup> )	rate, <sup>d</sup> 10 <sup>4</sup> (% s <sup>-1</sup> )	rate change <sup>e</sup>
Cabosil	DPP/2-FL	0.54/1.44	201 <sup>f</sup>	na
MCM-41 (2.8 nm)	DPP/2-FL	0.34/0.93	222	+10%
MCM-41 (1.6 nm)	DPP/2-FL	0.20/0.70	237	+18%
Cabosil	DPP/3-FL	0.39/1.08	82 <sup>f</sup>	na
MCM-41 (2.8 nm)	DPP/3-FL	0.30/0.80	181	+121%
MCM-41 (1.6 nm)	DPP/3-FL	0.18/0.53	268	+227%

<sup>a</sup> Cabosil is nonporous with a surface area of 200 m<sup>2</sup> g<sup>-1</sup>. Pore diameters for MCM-41 samples are in parentheses. <sup>b</sup> DPP = 1,3-diphenylpropane; FL = fluorene. <sup>c</sup> Density of grafted organic groups (molecules per nm<sup>2</sup> surface area) corrected for the mass of the organics. <sup>d</sup> Rate of DPP conversion obtained from the slopes of linear regressions of DPP versus reaction time based on 5–8 pyrolyses for each sample (DPP conversion range of 7–48%). Correlation coefficients for the regressions were 0.992–0.999. <sup>e</sup> Relative to corresponding Cabosil sample. <sup>f</sup> Data from ref 12.

bound styrene were detected in small amounts (3–7%) similar to that found previously in the Cabosil case.<sup>12</sup> Organic mass balances were quantitative within  $\pm 3\%$ .

## Results and Discussion

MCM-41 silicas with two different pore diameters of 2.8 and 1.6 nm were synthesized by standard methods.<sup>7</sup> Two-component mixtures of DPP and either 3-fluorene (3-FL) or 2-fluorene (2-FL) attached to these MCM-41 silicas (Figure 3a) were prepared at saturation surface coverages from the corresponding phenols by condensation with the surface silanols in a single step. Molecular grafting densities for these samples, which are normalized for differences in the silica surface areas and corrected for the masses of the organics, are given in Table 1. The FL/DPP ratios for these samples are comparable and in the range of 2.7–3.5. Prior studies on Cabosil showed that for several hydroaromatic spacer molecules, the DPP pyrolysis rates were similar for spacer/DPP ratios in the range of 2–7.<sup>12</sup> We note that the total organic grafting density for DPP plus spacer molecule is lower in the MCM-41 than on Cabosil, and it is further reduced at the smaller pore size consistent with our prior

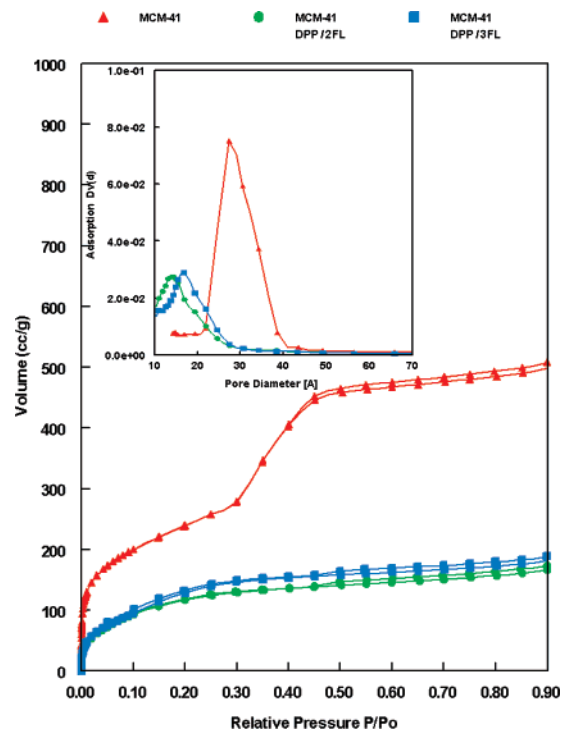


**Figure 4.** Nitrogen physisorption analysis of MCM-41 (2.8 nm) and its derivatives. Insert shows BJH pore size distribution.

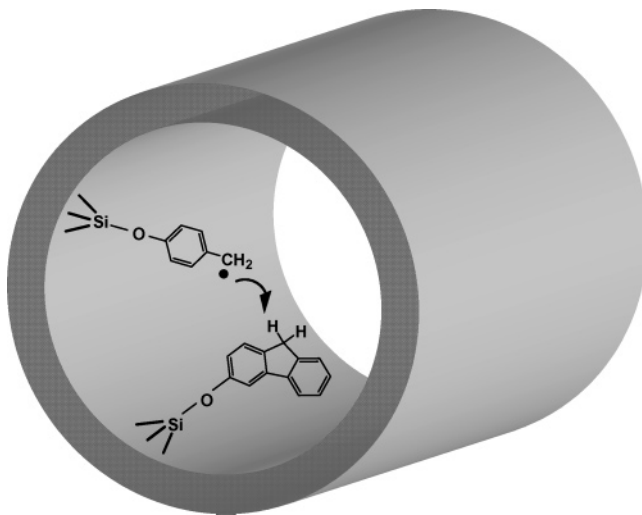


**Figure 5.** Illustration of MCM-41 concave cylindrical pore surface impacting the hydrogen transfer step for the 3-fluorene spacer molecule.

results.<sup>7–9</sup> The saturation grafting densities for DPP/3-FL samples are smaller than for the DPP/2-FL independent of the silica employed, indicating less efficient packing on the surface for the 3-FL isomer. Results from the BET analysis of the 2.8 nm MCM-41 sample and the two derivatives are shown in Figure 4 and Table 2. The decreases in pore size, surface area, and pore volume for the two-component derivatives are similar to those observed for saturation coverages of DPP alone.<sup>7</sup> The decreases in pore size, etc., are slightly less for the 3-FL isomer, consistent with the lower grafting density on the surface relative to the 2-FL isomer.

Pyrolysis studies were conducted at 375 °C under vacuum, and results are based on 5–8 runs for each sample. The same products were detected as shown in Figure 1a. The relative yields of gas-phase toluene and styrene provide a measure of possible regioselectivity in the reaction resulting from competitive hydrogen transfer steps 1a and 1b (Figure 1b). The benzylic

**TABLE 2: Comparison of Nitrogen Physisorption Data for Organic Derivatives of MCM-41 (2.8 nm)**

derivative	graft density <sup>a</sup> (nm <sup>-2</sup> )	pore diameter <sup>b</sup> (nm)	surface area <sup>c</sup> (m <sup>2</sup> g <sup>-1</sup> )	pore volume (cm <sup>3</sup> g <sup>-1</sup> )
none	na	2.8	913	0.94
DPP/2-FL	0.34/0.93	1.4	453	0.41
DPP/3-FL	0.30/0.80	1.7	515	0.44

<sup>a</sup> See Table 1. <sup>b</sup> BJH mean pore diameter. <sup>c</sup> BET specific surface area.

radical formed in step 1a should be slightly favored since it is para to the silyloxy linkage that is slightly stabilizing.<sup>15</sup> In the Cabosil case, this results in about a 10% excess in the toluene to styrene ratio.<sup>12a</sup> However, in the MCM-41 silicas, this ratio is nearly unity, suggesting that the benzylic hydrogen farthest from the surface tether is a bit more accessible in the nanoporous environment.

The DPP pyrolysis rates were obtained from the slopes of linear regressions of plots of DPP conversion versus reaction time, and they are reported in Table 1 along with those obtained previously on Cabosil. The differences between the 2-FL and the 3-FL spacers are striking. For DPP/2-FL, the reaction rate is slightly increased (10%) in the MCM-41 (2.8 nm pore size) compared with the corresponding reaction on Cabosil, and a further small rate increase is observed in the smaller pore size MCM-41 (1.6 nm). However, for the DPP/3-FL case, the reaction rate substantially increases by 121% for the MCM-41 with 2.8 nm pore size and 227% for the 1.6 nm pore size.

The DPP pyrolysis rate in the presence of hydrogen donor spacer molecules depends on the critical rate-determining steps in which hydrogen is transferred from the spacer molecules to the chain carrying gas-phase and surface-bound benzyl radicals, which was demonstrated in the prior studies on Cabosil.<sup>12,13</sup> For example, a full kinetic isotope effect of 2.7 was measured at 375 °C when PhCD<sub>2</sub>Ph was used as the spacer compared with PhCH<sub>2</sub>Ph.<sup>13</sup> In addition, when a set of spacer molecules with varying structures was investigated, the DPP pyrolysis rate was found to correlate with the hydrogen-donating ability of the spacer molecule to benzyl radicals as measured by solution-phase rate constants.<sup>12a</sup> In the current study, the origin of the rate differences between the two fluorene isomers most likely arises from the bimolecular hydrogen transfer step occurring on the surface (Figure 3b), since it appears unlikely that the mobile gas-phase benzyl radical would experience a significant sensitivity to the orientation of the fluorene spacer.

On the basis of thermochemical grounds, it is expected that the 3-FL isomer would produce a slightly faster rate since the radical formed following hydrogen transfer is para to the silyloxy linkage which is mildly stabilizing.<sup>12,15</sup> However, in the Cabosil case, the rate is considerably faster for the 2-FL isomer that contains a meta-linkage relative to the radical that is formed. The hydrogen transfer steps shown in Figure 3b are occurring on the relatively flat surface of these nonporous, low fractal dimension silica nanoparticles.<sup>12a</sup> We have modeled this hydrogen transfer step using the flat [111] surface of  $\beta$ -cristobalite as a model silica surface.<sup>12a</sup> The molecular modeling revealed that 2-FL is better able to attain a favorable distance and geometry for hydrogen transfer to the surface-attached, para-linked benzyl radical than is the 3-FL isomer. This was also observed for other hydrogen-donating spacer molecules such as 9,10-dihydrophenanthrene. The substantial rate increase observed in the mesoporous silicas for the 3-FL isomer must, therefore, be a consequence of improved orientation for bimolecular hydrogen transfer on the concave inner surface of the

cylindrical pore walls present in MCM-41<sup>16</sup> as illustrated in Figure 5. It is also possible that subsequent hydrogen transfer steps between the intermediate fluorenyl radicals and other fluorene and DPP molecules in the radical relay process are also facilitated on the pore surface. It is interesting that the rate is much faster in the 1.6 nm diameter pore sample of MCM-41 compared with the larger 2.6 nm pore sample. Prior studies of the pore size dependence of pyrolysis rates for DPP alone at saturation grafting densities showed only a ca. 15% increase in rate for similar changes in pore size.<sup>7a</sup> In the current case, this more noticeable pore size effect suggests that, in the smaller pore size MCM-41 where the radius of curvature of the pore wall is increased, additional improvements in the mutual molecular orientation for hydrogen transfer on the surface occur. In fact, in the 1.6 nm pore MCM-41, the pyrolysis rate is actually now faster (13%) for the 3-FL isomer than for 2-FL. This result would be consistent with thermochemical predictions in the absence of any orientation constraints.

## Conclusions

This research has provided new insights into the impacts of surface and pore confinement on free-radical reactions. The hydrogen transfer, radical relay pathway originally discovered for pyrolysis of diphenylpropane covalently attached to the external surface of nonporous Cabosil silica in the presence of coattached hydrogen-donating spacer molecules such as fluorene remains operative in the nanoporous environment of MCM-41 silica. However, the pyrolysis rate depends on both the orientation of the attached hydrogen donor and on the pore size of the MCM-41. Interestingly, while the presence of a meta-linked fluorene spacer molecule leads to a faster DPP pyrolysis rate on Cabosil compared with a para-linked fluorene, the opposite result is observed inside a 1.6 nm pore size MCM-41. The results indicate that the orientation constraints for efficient hydrogen transfer experienced by the para-linked fluorene on the exterior surface of Cabosil are mitigated or eliminated inside the MCM-41 mesoporous silicas. This suggests that pore confinement and surface curvature may play an important role in chemical transformations occurring for molecules confined to solid supports. In particular, bimolecular reactions in nanoporous solids could be sensitive to both pore size and surface orientation of the confined molecules, providing an additional means for controlling selectivity in chemical transformations.

**Acknowledgment.** This research was sponsored by the Division of Chemical Sciences, Geosciences, and Biosciences, Office of Basic Energy Sciences, U.S. Department of Energy, under contract DE-AC05-00OR22725 with Oak Ridge National Laboratory, managed and operated by UT-Battelle, LLC.

## References and Notes

- Huck, W. T. S. *Chem. Commun.* **2005**, 4143.
- Slowing, I.; Trewyn, B. G.; Lin, V. S.-Y. *J. Am. Chem. Soc.* **2006**, *128*, 14794.
- Li, C.; Zhang, H.; Jiang, D.; Yang, Q. *Chem. Commun.* **2007**, 547.
- Balas, F.; Manzano, M.; Horcajada, P.; Vallet-Regi, M. *J. Am. Chem. Soc.* **2006**, *128*, 8116.
- Houghten, R.; Yu, Y. *J. Am. Chem. Soc.* **2005**, *127*, 8582.
- Zhang, R.; Ding, W.; Tu, B.; Zhao, D. *Chem. Mater.* **2007**, *19*, 4379.
- (a) Kidder, M. K.; Britt, P. F.; Zhang, Z.; Dai, S.; Haganan, E. W.; Chaffee, A. L.; Buchanan, A. C., III *J. Am. Chem. Soc.* **2005**, *127*, 6353. (b) Kidder, M. K.; Britt, P. F.; Zhang, Z.; Dai, S.; Buchanan, A. C., III *Chem. Commun.* **2003**, 2804.
- Kidder, M. K.; Britt, P. F.; Buchanan, A. C., III *Energy Fuels* **2006**, *20*, 54.

- (9) Kidder, M. K.; Britt, P. F.; Chaffee, A. L.; Buchanan, A. C., III *Chem. Commun.* **2007**, 52.
- (10) Lin, H.-P.; Mou, C.-Y. *Acc. Chem. Res.* **2002**, 35, 927.
- (11) Anwender, R. *Chem. Mater.* **2001**, 13, 4419.
- (12) (a) Buchanan, A. C., III; Kidder, M. K.; Britt, P. F. *J. Phys. Chem. B* **2004**, 108, 16772. (b) Buchanan, A. C., III; Kidder, M. K.; Britt, P. F. *J. Am. Chem. Soc.* **2003**, 125, 11806.

- (13) Buchanan, A. C., III; Britt, P. F.; Thomas, K. B.; Biggs, C. A. *J. Am. Chem. Soc.* **1996**, 118, 2182.
- (14) Anwender, R.; Nagl, I.; Widenmeyer, M.; Engelhardt, G.; Groeger, O.; Palm, C.; Roser, T. *J. Phys. Chem. B* **2000**, 104, 3532.
- (15) Creary, X. *Acc. Chem. Res.* **2006**, 39, 761.
- (16) Ying, J. Y.; Mehnert, C. P.; Wong, M. S. *Angew. Chem., Int. Ed.* **1999**, 38, 56.